A Simple Numerical Algorithm and Software for Solution of Nucleation, Surface Growth, and Coagulation Problems

A. Prakash , A. P. Bapat & M. R. Zachariah

A Simple Numerical Algorithm and Software for Solution of Nucleation, Surface Growth, and Coagulation Problems

A. Prakash, A. P. Bapat, and M. R. Zachariah
Departments of Mechanical Engineering and Chemistry, University of Minnesota, Minneapolis, Minnesota

    In this article, a simple numerical method to solve the general dynamic equation (GDE) has been described and the software made available. The model solution described is suitable for problems involving gas-to-particle conversion due to supersaturation, coagulation, and surface growth of particles via evaporation/condensation of monomers. The model is based on simplifying the sectional approach to discretizing the particle size distribution with a nodal form. The GDE developed here is an extension of the coagulation equation solution method developed by Kari Lehtinen, wherein particles exist only at nodes, as opposed to continuous bins in the sectional method. The results have been tested by comparison where simple analytical solutions are available, and are shown to be in excellent agreement. By example we apply the model to the formation and growth of Aluminum particles. The important features of the model are that it is simple to comprehend; the software, which we call nodal GDE solver (NGDE), is relatively compact; and the code is well documented internally, so that users may apply it to their specific needs or make modifications as required. The C files mentioned in this article are available online at http://taylorandfrancis.metapress.com/openurl.asp?genre=journal&issn=0278-6826. To access this file, click on the link for this issue, then select this article. In order to access the full article online, you must either have an institutional subscription or a member subscription accessed through www.aaar.org.

INTRODUCTION

    The general dynamic equation (GDE) is the central continuity equation for aerosols, and its solution as such has received considerable attention. Because the GDE is a nonlinear, partial integro-differential equation, analytical solutions are available for only a few special cases (Gelbard and Seinfeld

1979; Peterson et al. 1978). Analytical studies on coalescence for different schemes of collision frequencies have been done by Scott (1968). Several approaches to solve the GDE numerically have been developed over the years. The most employed general method and its variants for simulating aerosol dynamics is based on dividing the particle size domain into sections as developed by Gelbard et al. (1980). The "J-Space" method (Suck and Brock 1979) also produces accurate results; however, the method may cause problems on inclusion of condensation (Williams and Loyalka 1991). For different representations of the size distribution function, simulations of coagulation and diffusion-limited condensation problems have been compared by Seigneur et al. (1986). Such problems involving coagulation and condensation have also been solved using hybrid (moving and stationary) size grid approach (Jacobson and Turco 1995). A widely used alternative approach has been the method of moments (e.g., Pratisinis 1988), which approximates the size distribution by a unimodal lognormal function.

    In this article, a simple approach has been proposed to solve the GDE for nonreactive systems which was developed as part of a graduate course project. The purpose of this article is not to compare the method's advantage over the many schemes available, but rather to indicate the simplicity of the algorithm and to offer the NGDE software for use by others. Essentially, it is a modification of the sectional method developed by Gelbard (1980) and an extension of a coagulation nodal method by Lehtinen and Zachariah (2001). In the sectional method the particle size domain is discretized into finite-sized sections. In the nodal method presented here, the finite-sized sections of the sectional model have been reduced to discrete points called "nodes" on the size domain. It is assumed that particles exist only at these nodes, which are evenly spaced on a logarithmic size scale. This assumption simplifies the computation by limiting the number of parameters.

    In the next section, the development of the model is shown. The underlying assumptions of the model are stated and the governing equations for the same are derived. The following section discusses the specific aerosol system, aluminum, for which the

model has been tested. Results for the specific problem have been presented and analyzed and a comparison with other approaches has been conducted to evaluate the method. In addition to verifying the reliability of results, the inherent errors introduced due to size splitting of particles into "zero-width" nodes have been examined in the final section.

MODEL DEVELOPMENT

Based on the sectional model approach a nodal form of the size distribution has been assumed wherein the total volume range for the aerosol is divided into nodes as opposed to discrete sections. In other words, the bins of finite width in the sectional model have been squeezed to zero width nodes in the nodal method, with the constraint that particles reside only at the nodes. Generally, in an aerosol system the particle sizes range from ~ 1 nm to about 10 μm. On the volume scale this size range corresponds to $\sim 10^{-27}$ m^3 to $\sim 10^{-15}$ m^3. To cover the 12 orders of magnitude for the volume range, the nodes are spaced linearly (with equal spacing) on a logarithmic scale. We have used a geometric spacing factor of 2 for the logarithmic volume scale. Using a geometric spacing factor of less than 2 would increase the accuracy; however, computational requirements increase substantially, with only a small increase in accuracy. With the above geometric factor, there are 10 size nodes per order of magnitude in the particle diameter space. In order to cover the above particle size range, 40 size nodes are required. Figure 1 illustrates the division of nodes on a logarithmic scale.

General Dynamic Equation

In writing the population balance, we limit the phenomena of interest to nucleation, coagulation, and surface growth.

$$v_i = q \times v_{i-1}$$

$$v_1 \quad v_2 \quad v_3 \quad v_4 \quad \text{log scale} \longrightarrow \quad v_{n-1} \quad v_n$$
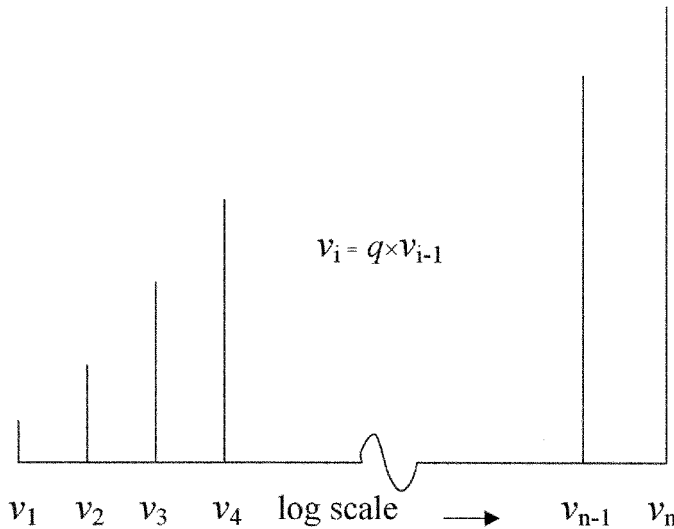
Figure 1. Illustration of node spacing on a logarithmic volume space where q is the geometric spacing factor, which in the present case is 2. The heights of the nodes correspond to the volume of the node (not drawn to scale).

Thus, the GDE is given by

$$\frac{dN_k}{dt} = \frac{dN_k}{dt}\bigg|_{coag} + \frac{dN_k}{dt}\bigg|_{nucl} + \frac{dN_k}{dt}\bigg|_{evap/cond}, \quad [1]$$

where N_k is the number concentration of particles at node k.

Nucleation

Gas-to-particle conversion occurs due to condensation of supersaturated vapor, and while several theories have been developed to model nucleation of particles, the model developed here uses classical homogenous nucleation theory with the self-consistent correction (SCC) proposed by Girshick and Chiu (1990):

$$J_k = n_s^2 S v_1 \left(\frac{2\sigma}{\pi m_1}\right)^{0.5} \exp\left(\theta - \frac{4\theta^3}{27\log^2 S}\right). \quad [2]$$

Nucleation leads to the production of particles of critical size (v^*), which may happen to occur at a node or more likely between two nodes. Since the particles reside only at the nodes, particles nucleated between two nodes are put in the next higher node. Conservation of particle volume is accounted for by multiplying the nucleated volume by a size operator ξ_k given below. This process of putting the nucleated particles at the node just larger than k* is shown in Figure 2. Note that node 1 corresponds to the monomer units and nodes 2 through 40 are considered clusters, of which the ones that are larger than k* are termed "particles".

$$\xi_k = \begin{cases} \dfrac{v^*}{v_k}; & \text{if } v_{k-1} \leq v^* \leq v_k, \\[2mm] \dfrac{v^*}{v_2}; & \text{if } v^* \leq v_1, \\[2mm] 0; & \text{otherwise.} \end{cases} \quad [3]$$

Thus the population change due to nucleation is

$$\frac{dN_k}{dt}\bigg|_{nucl} = J_k(t)\xi_k. \quad [4]$$

Coagulation

Collision of two particles larger than the critical size node k* is termed "coagulation." In the development of this model free molecular regime has been assumed for the calculation of collision frequency function. Although most of the nodes reside in the free molecular regime, there are particles that reside in the transition regime as well ($d_p \sim \lambda$). It is important to note that mean free path of a carrier gas molecule at temperature range being studied here is on the order of a fraction of a μm. Also, growth of particles due to condensation and evaporation processes have much smaller characteristic time as compared to coagulation, so as the particles grow coagulation has little role to play. The comparative contribution of coagulation and growth has been described in the results section (Figure 9). The
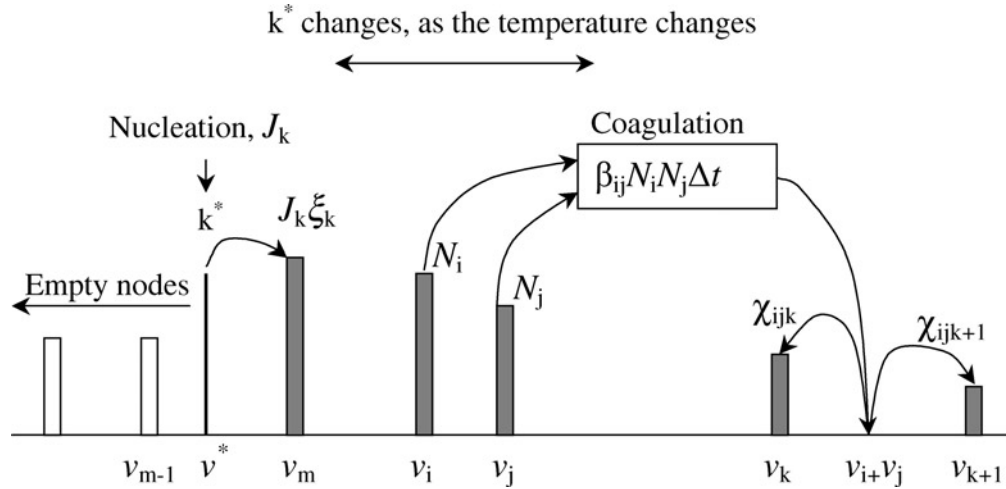
Figure 2. Illustration of the GDE algorithm. Nucleation occurs at the node just larger than the critical cluster size. k^* moves on the volume space due to changes in saturation ratio. Splitting of particles formed from coagulation of particles of sizes v_i and v_j into nodes adjacent to $v_i + v_j$ is also shown.

collision frequency function $\beta(v_i, v_j)$ for collision of particles of volumes v_i and v_j is given by (Friedlander 2000)

$$\beta(v_i, v_j) = \left(\frac{3}{4\pi}\right)^{1/6}\left(\frac{6kT}{\rho_p}\right)^{1/2}\left(\frac{1}{v_i} + \frac{1}{v_j}\right)^{1/2}\left(v_i^{1/3} + v_j^{1/3}\right)^2.$$
[5]

The above assumption holds good for most cases; however, for a more accurate calculation on collision rates one can use Fuchs form of collision coefficient (Seinfeld and Pandis 1998), and such a provision is available in the NGDE program. The rate of change of particle size distribution (PSD) due to coagulation is given by a modified Smoluchowski equation:

$$\left.\frac{dN_k}{dt}\right|_{coag} = \frac{1}{2}\sum_{\substack{i=2\\j=2}} \chi_{ijk}\beta_{i,j}N_iN_j - N_k\sum_{i=2}\beta_{i,k}N_i.$$
[6]

Particles of volume v_i and v_j collide, resulting in a particle of volume $v_i + v_j$. If this volume falls between two nodes, the new particle is split into adjacent nodes (Figure 2) under the constraint of mass conservation. Thus we define a size-splitting operator χ_{ijk} as follows:

$$\chi_{ijk} = \begin{cases} \dfrac{v_{k+1} - (v_i + v_j)}{v_{k+1} - v_k}; & \text{if } v_k \leq v_i + v_j \leq v_{k+1}, \\ \dfrac{(v_i + v_j) - v_{k-1}}{v_k - v_{k-1}}; & \text{if } v_{k-1} \leq v_i + v_j \leq v_k, \\ 0; & \text{otherwise.} \end{cases}$$
[7]

Surface Growth

Particles either grow due to condensation of monomers or shrink due to evaporation of monomers from the surface. The driving force for condensation or evaporation depends on the dif-

ference between the vapor pressure of monomer and the Kelvin effect adjusted saturation vapor pressure for the particular particle size of interest.

A particle may be added to a node either due to condensation of monomers on smaller particles or evaporation from larger particles. Likewise, a particle may be removed from a node due to either its evaporation to a smaller size node or the condensation of monomers to form a larger particle. The change in PSD due to evaporation or condensation of monomers can be mathematically expressed as

$$\left.\frac{dN_k}{dt}\right|_{evap/cond}$$

$$= \begin{cases} \dfrac{v_1}{v_k - v_{k-1}}\beta_{1,k-1}\left(N_1 - N_{1,k-1}^s\right)N_{k-1} & \text{if } N_1 > N_{1,k-1}^s, \\ -\dfrac{v_1}{v_{k+1} - v_k}\beta_{1,k+1}\left(N_1 - N_{1,k+1}^s\right)N_{k+1} & \text{if } N_1 < N_{1,k+1}^s, \\ -\dfrac{v_1}{v_{k+1} - v_k}\beta_{1,k}\left(N_1 - N_{1,k}^s\right)N_k & \text{if } N_1 > N_{1,k}^s, \\ \dfrac{v_1}{v_k - v_{k-1}}\beta_{1,k}\left(N_1 - N_{1,k}^s\right)N_k & \text{if } N_1 < N_{1,k}^s. \end{cases}$$
[8]

Monomer Balance

Monomers are involved in nucleation and surface growth of particles. A monomer balance is necessary to account for monomer concentration changes due to nucleation, condensation, and evaporation:

$$\frac{dN_1}{dt} = \left.\frac{dN_1}{dt}\right|_{nucl} + \left.\frac{dN_1}{dt}\right|_{evap/cond},$$
[9]

where

$$\left.\frac{dN_1}{dt}\right|_{nucl} = -J_k k^*, \qquad [10]$$

$$\left.\frac{dN_1}{dt}\right|_{evap/cond}$$
$$= \begin{cases} -\beta_{1,k-1}\left(N_1 - N_{1,k-1}^s\right)N_{k-1} & \text{if } N_1 > N_{1,k-1}^s, \\ -\beta_{1,k+1}\left(N_1 - N_{1,k+1}^s\right)N_{k+1} & \text{if } N_1 < N_{1,k+1}^s, \\ -\beta_{1,k}\left(N_1 - N_{1,k}^s\right)N_k & \text{if } N_1 > N_{1,k}^s, \\ -\beta_{1,k}\left(N_1 - N_{1,k}^s\right)N_k & \text{if } N_1 < N_{1,k}^s. \end{cases} \qquad [11]$$

RESULTS AND DISCUSSION

By way of demonstrating the use of the model we apply it to the problem of aluminum particle formation and growth from a vapor at 1773 K as it is passed into a condenser, with a cooling rate of 1000 K/s. The problem conditions for these tests were adapted from an earlier work by Panda and Pratsinis (1995) on the modeling of evaporation-condensation of aluminum in an aerosol flow reactor. Below we test each of the three modules of the GDE and present the unified model. To illustrate the solution of the example problem, the free molecular regime ($d_p \ll \lambda$) has been assumed for the calculation of the collision frequency function.

Coagulation

We evaluate the accuracy of the coagulation module against Friedlander and Wang's (1966) similarity transformation for the size distribution function. Friedlander showed that for a purely coagulating aerosol the resulting particle size distribution (PSD) becomes asymptotically (at long time) independent of the initial conditions. These asymptotic distributions are independent of time when plotted in a nondimensional form as shown by Friedlander (2000) and are termed as "self-preserving distributions"(SPD). We compare our results with those obtained by the discrete-sectional method of Vemury et al. (1994) using an initially monodisperse aerosol. As seen in Figure 3, we find very good agreement between the SPD computed by the two techniques.

Nucleation and Coagulation

The variation in size distribution with time with just the nucleation and coagulation modules of the GDE turned on is presented in Figure 4. The distribution function evolves into an approximately lognormal form. The node at which nucleation of particles would occur is determined by the critical cluster size, k*. Figure 5 shows the variation of k* with time. As the system cools down, k* shifts towards smaller nodes and the number of particles added at a node due to nucleation depends on the nucleation rate. Figure 4 shows the evolution of the size distribution
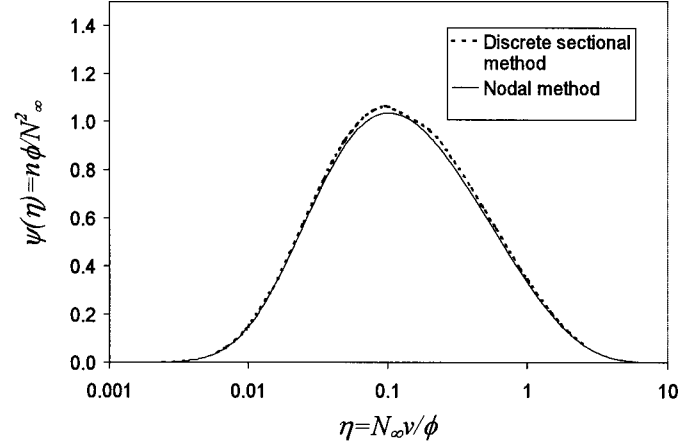
Figure 3. Self-preserving particle size distribution in the free molecular regime, compared with values calculated by a discrete sectional method (Vemury et al. 1994).

with time, and it appears that particles coagulate to increase in size while the number concentration of particles in the smaller sized nodes falls. However, the high concentration of particles that we see at the still smaller nodes is due to nucleation. At long times, k* is very small and particles are continuously being added in the smallest node due to nucleation.

Surface Growth

As normally formulated, the critical particle volume v^* is the particle volume at which nucleation occurs. In the present model, it is modified to reside at the next larger node as it is unlikely that v^* would happen to occur at an existing node. Particles
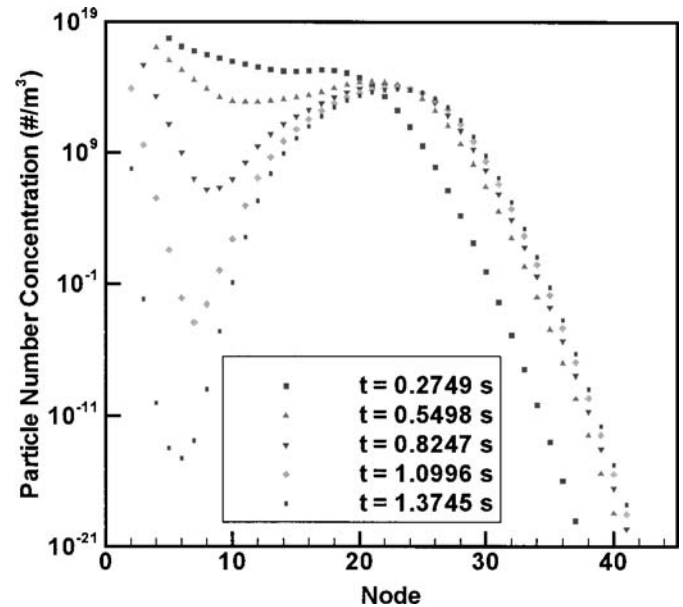
Figure 4. Evolution of size distribution due to nucleation and coagulation.
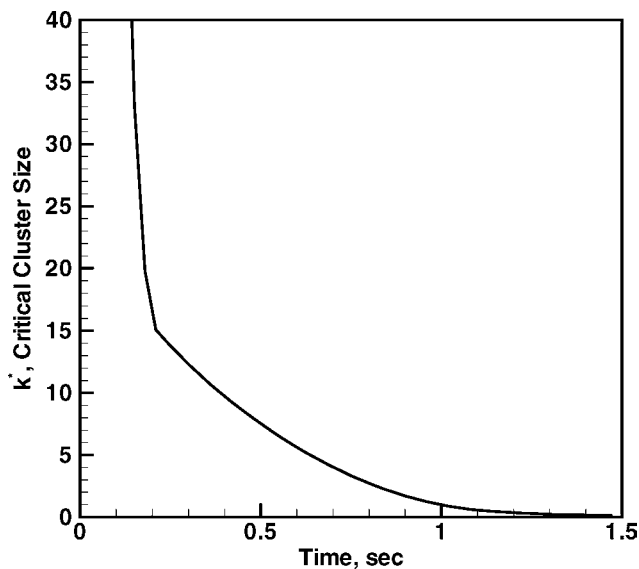
Figure 5. Variation of critical cluster size (k*) with time as the system cools.

with volume less than v^* have a tendency to evaporate, whereas those with size larger than v^* tend to grow. To test the model for pure surface growth, a monodisperse aerosol of concentration 10^{10} m^{-3} was added at node 25 and the change in PSD with time is shown in Figure 6. The monomer concentration was fixed to test the growth module. At later times as surface growth occurs particles move into adjacent nodes depending on the critical size v^* which determines at each time step whether the particles at
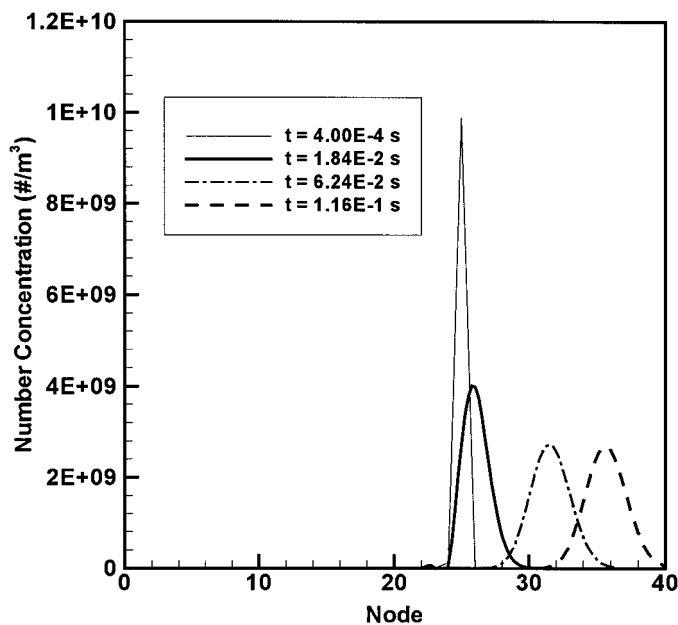
a particular node will grow or evaporate. In our test problem shown in Figure 6 particle growth is observed because, as the system cools, k* decreases.

The Complete GDE

The model was finally tested for the complete GDE. In this model, the system has been restricted to a size range from the 0.3 nm to 3.25 μm. Though the probability of collision of large particles is very low, coagulation may still lead to formation of a few particles beyond the largest node. In order to account for the mass conservation, these particles are put into the largest node. However, it is important to note that the number of such particles is small enough not to affect the PSD.

The PSD obtained from the solution of the complete GDE is shown in Figure 7, while Figure 8 shows the variation in the nucleation rate J_k and saturation ratio S. For the conditions here, the nucleation rate peaks at about 0.14 s. Figures 7–9 are closely correlated. Figure 7 shows the burst of new particles, which corresponds to the peak in the nucleation rate. Nucleation of particles occurs at larger nodes initially, so we do not see any particles in the smaller nodes (nodes smaller than 8). However, as k* moves towards smaller nodes, at later times the smaller nodes also get populated. Thereafter the PSD is shaped by coagulation and surface growth processes, which are slow compared to nucleation. The particle mean diameter presented in Figure 9 also increases after the initial nucleation burst (Figure 8). Recall that the node at which nucleation occurs is determined by the critical cluster size k*, the variation of which is similar to that shown in Figure 5. As the particles are created, the mean diameter increases due to coagulation and surface growth. The flattening of the particle mean diameter curve corresponds to slower
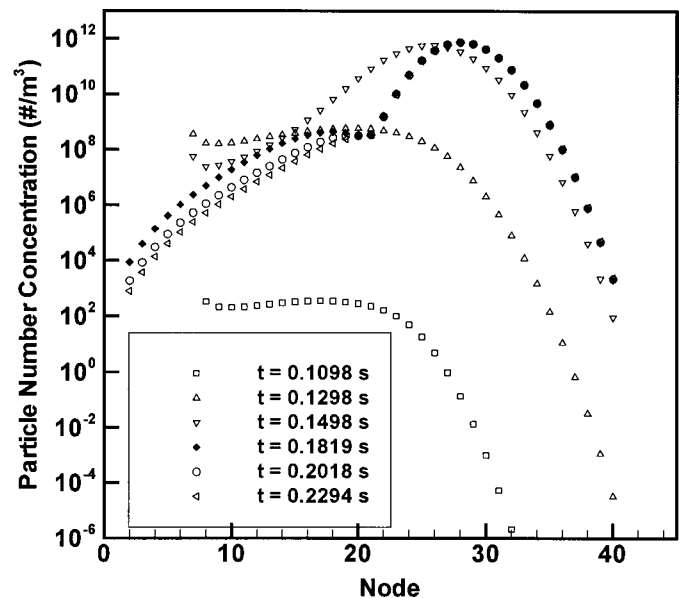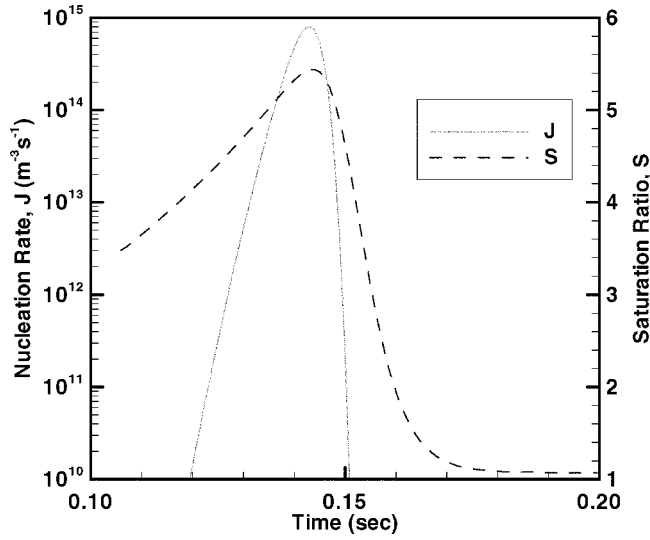

Figure 6. Pure surface growth causes a shift in PSD. Size distribution broadens with time due to size splitting of particles into adjacent nodes.

Figure 7. Variation of size distribution with time for the complete GDE.

**Figure 8.** Variation of nucleation rate and saturation ratio with time.

growth, dominated by heterogeneous nucleation. Figure 9 also shows the variation of total number concentration of particles with time. We notice that after about 0.15 s the number concentration is essentially constant, implying that new particle formation has ceased. Particle coagulation will decrease the number concentration; however, at the number densities produced here the characteristic half-life due to coagulation is on the order of minutes.

ERROR ANALYSIS

The size-splitting approach incorporates a discrete nodal structure for the volume space, which inherently introduces errors in the estimation of the distribution function. Agreement
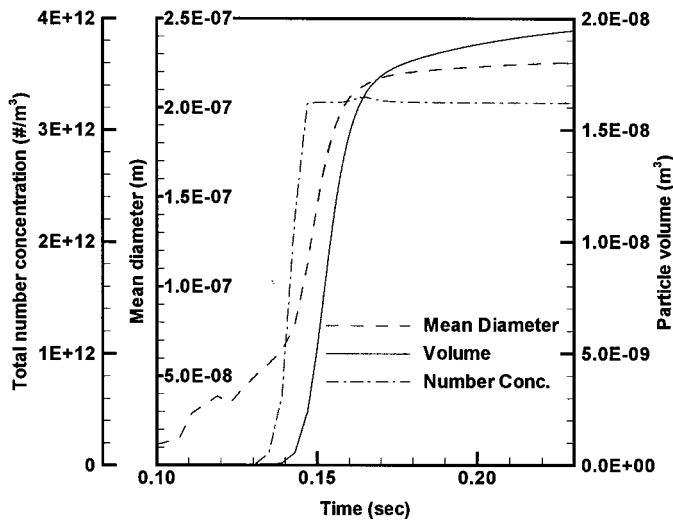
Figure 9. Variation of mean diameter, number concentration, and total particle volume with time.
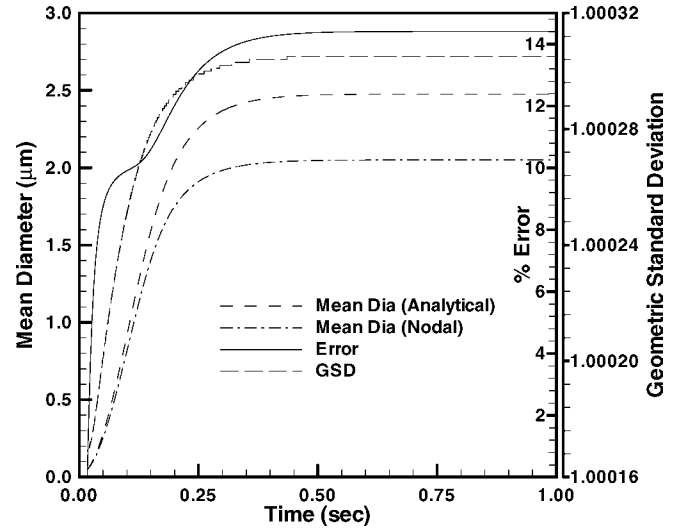
Figure 10. Comparison of mean diameters from the nodal solution and from the heterogeneous growth equation.

of the self-preserving distribution obtained from the model with the similarity solution of Friedlander validated the coagulation module. The effect of size splitting on nucleation is minimal, since the nucleation time scales are small (compared to surface growth) and thus errors do not accumulate over time. The error introduced due to surface growth process arising from size splitting was estimated by comparing the mean diameter predicted by the model with that obtained from the heterogeneous growth law (Friedlander 2000) given by

$$\frac{dv}{dt} = \frac{\pi d_p^2 v_m (p_1 - p_d)}{(2\pi mkT)^{1/2}}. \qquad [12]$$

The nucleation and coagulation modules of the model were turned off and the growth of a monodisperse aerosol was observed with time with 10^{10} particles/m^3 in node 20 (25 nm). The mean diameters (analytical and model) and the relative error are plotted in Figure 10. It is obvious that an initially monodisperse aerosol should remain monodisperse, as growth of all the particles occurs uniformly. However, we observe that an initially monodisperse aerosol becomes polydisperse, which is a direct consequence of size splitting and is thus a drawback of the nodal method. The geometric standard deviation (GSD) of the size distribution obtained from the nodal method has also been plotted in Figure 10. Note that the GSD of size distribution obtained from the analytical solution will be unity, since it always remains monodisperse. Using a larger number of nodes in the simulation can further reduce these deviations. It is also clear that the error increases with an increase in the mean diameter due to surface growth of particles. However, as the monomers deplete the growth process becomes less intense, resulting in flattening of the mean diameter curve and consequently limiting the error. A similar calculation done for 10^{20} particles/m^3 predicts maximum errors on the order of 0.1%. We see that with

an increase in the volume loading of aerosol (increase in number concentration of particles), the error is reduced for a given monomer loading. The number concentration of particles in the aerosol system considered here (and in general) is of order 10^{10} particles/m^3. Thus, the maximum error that can be introduced due to size splitting should not exceed $\sim$15%. However, repeated cycles of subsequent condensation and evaporation may cause the errors to accumulate. In such a case, larger number of nodes should be used to obtain more accurate results.

CONCLUSIONS

In this article, we have presented a simple numerical scheme to solve the GDE for problems involving classical nucleation, surface growth/evaporation, and coagulation. The algorithm and software were originally developed as part of a graduate course in Aerosol Dynamics. The methodology approximates the particle size distribution to a few nodes by introducing size-splitting operators. Examples for the growth of aluminum particles from the vapor were presented. The results have been compared with other models and show excellent agreement. The software NGDE should be readily usable and adaptable to other users' needs or as a teaching tool.

NOMENCLATURE

J_k	Nucleation rate, m^{-3} s^{-1}
k_b	Boltzmann constant, J/K
m_1	Mass of a monomer unit, Kg
n_s	Number concentration of monomers at saturation, m^{-3}
N_k/V_k	Number concentration/volume of particles at the kth node, m^{-3}/m^3
$N_{1,k}^s$	Number concentration of monomers over a k sized particle at saturation, m^{-3}
N_∞	Total number concentration of particles, m^{-3}
s_1	Surface area of a monomer unit, m^2
S	Saturation ratio
T	Temperature, K
v^*	Volume of the critical cluster size, m^3
v_1	Volume of a monomer unit, m^3

Greek Letters

θ	Nondimensional surface tension, $\theta = \frac{s_1\sigma}{k_b T}$
ρ_p	Mass density of particle, kg/m^3
σ	Surface tension, N/m

REFERENCES

Friedlander, S. K. (2000). *Smoke Dust and Haze*, Oxford Univ. Press, Oxford, p. 210.

Friedlander, S. K., and Wang, C. L. (1966). Self-Preserving Particle Size Distribution for Coagulation by Brownian Motion, *J. Colloid Interface Sci.* 22:126–132.

Gelbard, F., Tambour, Y., and Seinfeld, J. H. (1980). Sectional Representations for Simulating Aerosol Dynamics, *J. Colloid Interface Sci.* 76(2):541–556.

Gelbard, F., and Seinfeld, J. H. (1979). The General Dynamics Equation for Aerosols, *J. Colloid Interface Sci.* 68(2):363–382.

Girshick, S. L., and Chiu, Chia Pin. (1990). Kinetic Nucleation Theory: A New Expression for the Rate of Homogeneous Nucleation from an Ideal Supersaturated Vapor, *J. Chem. Phys.* 93:1273–1277.

Jacobson, M. Z., and Turco, R. P. (1995). Simulating Condensational Growth, Evaporation, and Coagulation of Aerosols Using a Combined Moving and Stationary Size Grid, *Aerosol Sci. Technol.* 22:73–92.

Lehtinen, K. E. J., and Zachariah, M. R. (2001). Self-Preserving Theory for the Volume Distribution of Particles Undergoing Brownian Coagulation, *J. Colloid Interface Sci.* 242:314–318.

Panda, S., and Pratsinis, S. E. (1995). Modeling the Synthesis of Aluminum Particles by Evaporation-Condensation in an Aerosol Flow Reactor, *Nano Structured Materials* 5:755–767.

Peterson, T. W., Gelbard, F., and Seinfeld, J. H. (1978). Dynamics of Source-Reinforced, Coagulating, and Condensing Aerosols, *J. Colloid Interface Sci.* 63:426–445.

Pratsinis, S. E. (1988). Simultaneous Nucleation, Condensation, and Coagulation in Aerosol Reactors, *J. Colloid Interface Sci.* 124(2):416–427.

Scott, W. T. (1968). Analytic Studies of Cloud Droplet Coalescence, *J. Atmos. Sci.* 25:54–65.

Seigneur, C., Hudischewskyj, A. B., Seinfeld, J. H., Whitby, K. T., Whitby, E. R., Brock, J. R., and Barnes, H. M. (1986). Simulation of Aerosol Dynamics: A Comparative Review of Mathematical Models, *Aerosol Sci. Technol.* 5:205–222.

Seinfeld, J. H., and Pandis, S. N. (1998). *Atmospheric Chemistry and Physics*, John Wiley & Sons, pp. 659–662.

Suck, S. H., and Brock, J. R. (1979). Evolution of Atmospheric Aerosol Particle Size Distributions via Brownian Coagulation: Numerical Simulation, *J. Aerosol Sci.* 10:581–590.

Vemury, S., Kusters, K. A., and Pratsinis, S. E. (1994). Time-lag for Attainment of the Self-Preserving Particle Size Distribution by Coagulation, *J. Colloid Interface Sci.* 165:53–59.

Williams, M. M. R., and Loyalka, S. K. (1991). *Aerosol Science: Theory and Practice*, Pergamon, Oxford.

APPENDIX

The numerical algorithm proposed in this article has been implemented in C. The example problem is specific for a growth of aluminum aerosol by the evaporation-condensation method; however, the software is designed to allow the user to apply it to other systems where property data such as saturation vapor pressures and surface tension are known. The program code performs four main types of calculations: (1) pure coagulation, (2) coupled nucleation and coagulation, (3) pure surface growth, and (4) unified GDE containing all of the above.

The program execution consists of the user inputting to the input file the necessary data about the aerosol material properties and the process conditions. The output can be either viewed on the console or directed to a file for storage.

The source code for the program has a modular structure. Each section of the code is independent of other sections. The source is well commented and a list of variable names and their units are documented within the code to allow the user to make customized changes.

The entire NGDE package provided consists of the source code in C, an instruction file readme.txt, and the sample input files for the example problem discussed in the article. The electronic version of the package is available for download (see abstract).